INSTITUTE OF PHYSICS PUBLISHING SEMICONDUCTOR SCIENCE AND TECHNOLOGY

Semicond. Sci. Technol. **20** (2005) L5–L9 doi:10.1088/0268-1242/20/3/L02

LETTER TO THE EDITOR

Magnetic and optical properties of $Ga_{1-x}Mn_xN$ grown by metalorganic chemical vapour deposition

M H Kane[1,2], A Asghar[2], C R Vestal[3], M Strassburg[4], J Senawiratne[4], Z J Zhang[3], N Dietz[4], C J Summers[1] and I T Ferguson[1,2]

[1] School of Materials Science and Engineering, Georgia Institute of Technology, Atlanta, GA 30332-0245, USA
[2] School of Electrical and Computer Engineering, Georgia Institute of Technology, Atlanta, GA 30332-0250, USA
[3] School of Chemistry and Biochemistry, Georgia Institute of Technology, Atlanta, GA 30332-0400, USA
[4] Department of Physics and Astronomy, Georgia State University, Atlanta, GA 30303-4106, USA

E-mail: ianf@ece.gatech.edu

Received 22 October 2004, in final form 17 January 2005
Published 17 February 2005
Online at stacks.iop.org/SST/20/L5

Abstract

Epitaxial layers of $Ga_{1-x}Mn_xN$ with concentrations of up to $x = 0.015$ have been grown on c-sapphire substrates by metalorganic chemical vapour deposition. No ferromagnetic second phases were detected via high-resolution x-ray diffraction. Crystalline quality and surface structure were measured by x-ray diffraction and atomic force microscopy, respectively. No significant deterioration in crystal quality and no increase in surface roughness with the incorporation of Mn were detected. Optical measurements show a broad emission band attributed to a Mn-related transition at 3.0 eV that is not seen in the underlying GaN virtual substrate layers. Room temperature ferromagnetic hysteresis has been observed in these samples, which may be due to either Mn-clustering on the atomic scale or the $Ga_{1-x}Mn_xN$ bulk alloy.

1. Introduction

The field of spintronics seeks to exploit both the electron spin and its charge in order to introduce an additional degree of freedom to the next generation of electronic devices. Diluted magnetic semiconductors (DMS) have attracted considerable interest as materials that can support the transport and storage of spin, and that can be integrated into existing electronic and optoelectronic devices. Traditional III–V ferromagnetic DMS, such as $Ga_{1-x}Mn_xAs$, suffer from the limitation that they only retain their ferromagnetism at cryogenic temperatures (<170 K), which precludes their practical use in room temperature devices. Subsequent predictions using the Zener mean-field model of ferromagnetism [1] predicted that room temperature (RT) ferromagnetism might be achieved in p-type III–V and II–VI materials with lower spin–orbit couplings and shorter bond lengths. GaN and ZnO doped with Mn or other transition metals are such materials, but it is necessary to maintain high ($>10^{20}$ cm^{-3}) hole concentrations [1]. This theory, however, has not been able to fully explain the observed ferromagnetism in the wide bandgap materials, nor has a wide bandgap material been produced with the properties required by the mean-field model for RT ferromagnetism. Subsequent theories for the ferromagnetism have been developed based on Mn clusters [2, 3] which do not necessarily require the presence of free carriers. Additional calculations suggest that

a double exchange mechanism may be suitable for stabilizing the ferromagnetic state in $Ga_{1-x}Mn_xN$ [4]. Other *ab initio* density functional theory calculations of the band structure of $Ga_{1-x}Mn_xN$ predict the formation of a Mn impurity-related sub-band in the bandgap [5] that could also be related to the ferromagnetism in these materials. Understanding the inherent mechanism in these materials is crucial for future device applications.

Recently, considerable effort has been devoted to producing $Ga_{1-x}Mn_xN$ that is ferromagnetic at RT. Several groups have reported ferromagnetism in $Ga_{1-x}Mn_xN$ produced by a number of different methods, including post-growth diffusion [6], ion implantation [7] and molecular beam epitaxy (MBE) [8, 9], with Curie temperatures (T_C) up to 940 K [9], depending on growth conditions. There are limited reports involving Mn incorporation into GaN films grown by metalorganic chemical vapour deposition (MOCVD) at dopant concentration levels [10]. The magnetic properties of MOCVD-grown $Ga_{1-x}Mn_xN$ with manganese concentrations necessary for DMS behaviour are largely unexplored in the literature. RT ferromagnetism in $Ga_{1-x}Mn_xN$ is still controversial, as the materials are insulating and do not exhibit magnetic circular dichroism [11], which is an indicator of mean-field DMS behaviour in $Ga_{1-x}Mn_xAs$. In addition, second phases such as GaMn or Mn_4N have been observed through transmission electron microscopy (TEM) and x-ray diffraction (XRD) in heavily-doped samples produced by MBE [12, 13]. These phases are sometimes attributed as the sole source of ferromagnetism in these materials. Furthermore, there is little evidence at this time to support the conclusion that the currently produced RT ferromagnetic films of $Ga_{1-x}Mn_xN$ have any coupling between the free carrier concentration (either in the valence or in the conduction band) and the magnetic centres, which would be required for practical spintronic applications.

Since MOCVD is generally regarded as the optimal technique for the growth of high quality III-nitrides, it is desirable to be able to produce ferromagnetic $Ga_{1-x}Mn_xN$ by this method. In this work, the MOCVD growth of $Ga_{1-x}Mn_xN$ films and the investigations on the structural, magnetic and optical properties are reported. A homogeneous depth distribution of Mn in the epilayers was confirmed via SIMS. Room temperature magnetic hysteresis was observed in samples with Mn concentrations as low as 1%. Manganese-related optical transitions were seen near 3.0 eV.

2. Experimental procedure

The growth was performed in a specially modified Veeco Discovery series D-125 GaN MOCVD tool with a vertical injection system into a short jar confined-inlet design using multiple switching injection blocks to minimize gas phase pre-reactions. Initially, undoped 1–2 μm thick MOCVD-grown GaN epilayers were used as templates on which to grow $Ga_{1-x}Mn_xN$ epilayers. Trimethyl gallium and ammonia were used as a source of gallium and nitrogen, while bis-cyclopentyldienyl manganese (Cp_2Mn) was used to dope the epilayers with manganese. A series of systemic runs were carried out at different temperatures ranging from 900 °C to 1050 °C and V/III ratios from 800 to 1100 to narrow down the optimum growth conditions to grow epilayers without phase segregation. Different Mn doping levels were achieved by changing the molar flow of Mn going into the reactor or by reducing the molar concentration of Ga to better control the Mn incorporation at different growth rates. A systematic growth study of the growth of $Ga_{1-x}Mn_xN$ to better understand the incorporation of Mn at higher concentrations than those used in this work will be reported elsewhere.

Five $Ga_{1-x}Mn_xN$ films are described here, (A: 300 nm, $x = 0.003$; B: 300 nm, $x = 0.005$; C: 1000 nm, $x = 0.01$; D: 1000 nm, $x = 0.012$; E: 1200 nm, $x = 0.015$). To provide a standard for comparison, samples of MOCVD-grown p-type ($p = 2 \times 10^{16}$ cm^{-3}) and intrinsic GaN were ion-implanted with Mn concentrations of 3×10^{16} cm^{-2} at an energy of 200 keV and a substrate temperature of 400 °C. In order to remove the implantation damage, samples were subsequently annealed by rapid thermal annealing (RTA). The samples were placed face-down on GaN templates in a flowing nitrogen atmosphere at temperatures ranging from 700 °C to 900 °C for 4 min. Crystalline quality and phase purity were determined by high-resolution XRD using a Philips X'Pert Pro MRD diffractometer. Atomic force microscopy (AFM) was performed using a PSIA XE-100. Magnetic properties were analysed using a Quantum Design MPMS 5S SQUID magnetometer at temperatures from 5 to 300 K. Secondary ion mass spectroscopy (SIMS) depth profiles were performed on the samples using an Atomika Instruments Ionmicroprobe A-DIDA 3000. Room temperature photoluminescence (PL) was performed using a frequency-doubled Ti:Sa laser at 356.5 nm as an excitation source. Optical transmission experiments were performed using a 75 W XBO lamp.

3. Results and discussion

The as-grown $Ga_{1-x}Mn_xN$ films were specular but had a distinct reddish-brown tinge, consistent with substitutional Mn transitions in GaN films and crystals produced by other methods [14]. AFM indicated a 2D step flow growth mode with a surface roughness of 3.78 Å in the most heavily doped film, which is close to that from the as-grown template layer of 3.30 Å. A ω–2θ high-resolution XRD scan from 20° to 60° is shown in figure 1; no macroscopic second phases are visible where the major peaks of the impurity phases have been previously observed [13, 15]. In addition, no noticeable shift in the lattice parameter is detected for these samples at low (<2%) Mn concentrations. The full width half maximum (FWHM) values of the ω–2θ scan for sample B were (002): 150 arcsec and (102): 522 arcsec, which are close to those of the GaN virtual substrate (179 and 518 arcsec, respectively). No secondary phases are observed in the as-grown samples up to doping levels of approximately 2%.

Depth profiles of two thin $Ga_{1-x}Mn_xN$ epilayer samples (A and B) recorded by SIMS are shown in figure 2. For the sake of comparison, the measured depth profile of a Mn^+ ion implanted sample with an implantation dose of 3×10^{16} cm^{-2} at 200 keV is depicted. In contrast to the implanted samples, a uniform Mn concentration with depth is confirmed for the MOCVD grown samples. The Mn concentrations obtained from the spectra in figure 2 are $x = 0.003$ and $x = 0.005$ for samples A and B, respectively. The layer thicknesses

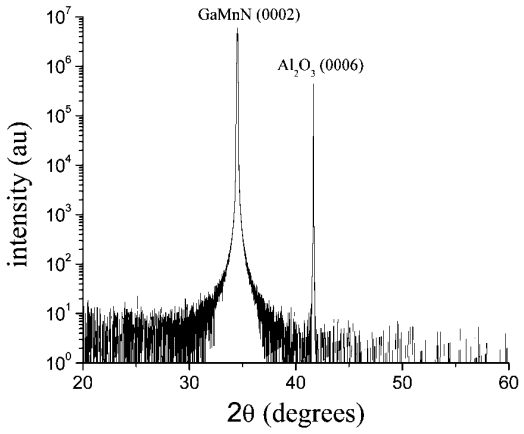

Figure 1. 2θ–ω XRD diffraction scan of $Ga_{1-x}Mn_xN$ sample D ($x = 0.012$) from 20°–60° showing no second phase formation in the MOCVD-grown films.

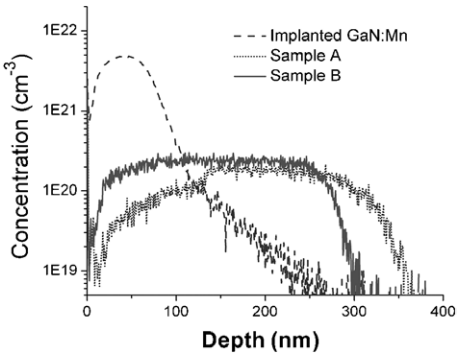

Figure 2. SIMS profile for Mn-55 of implanted and MOCVD-grown $Ga_{1-x}Mn_xN$ samples A ($x = 0.003$) and B ($x = 0.005$). In the MOCVD-grown films, a uniform depth distribution of Mn is seen in the layers.

determined by SIMS are 250 nm and 300 nm respectively, matching those derived from the *in situ* reflectometry during the growth. For samples C, D and E, SIMS yielded concentrations of $x = 0.01$, $x = 0.012$ and $x = 0.015$ respectively, though exact quantification via SIMS in these samples is difficult due to the high lattice concentrations of the Mn.

Optical studies are essential to examine possible defect states and formation of impurity bands from the introduction of manganese, as the lattice-site incorporation of Mn is essential for the development and application of these materials. Further information about the Mn incorporation is obtained by optical spectroscopy and comparison with the extensive studies in the literature. Figure 3 shows the photoluminescence (PL) behaviour of the thicker, more heavily doped sample C both before and after annealing. In this sample, the most prominent feature is the blue emission band around 3.0 eV which is also reported in both ion-implanted and MBE-grown $Ga_{1-x}Mn_xN$. Transitions from conduction band electrons to Mn-related states and from shallow donor (e.g., N vacancy) to Mn acceptor states are assigned to cause these emission bands in the respective spectral range, as has been previously suggested [7, 16–18]. Peak energies reported for this emission band range from 2.90 eV [7] through 3.08 eV [19] at room temperature. Lifetime measurements suggest similarity to the

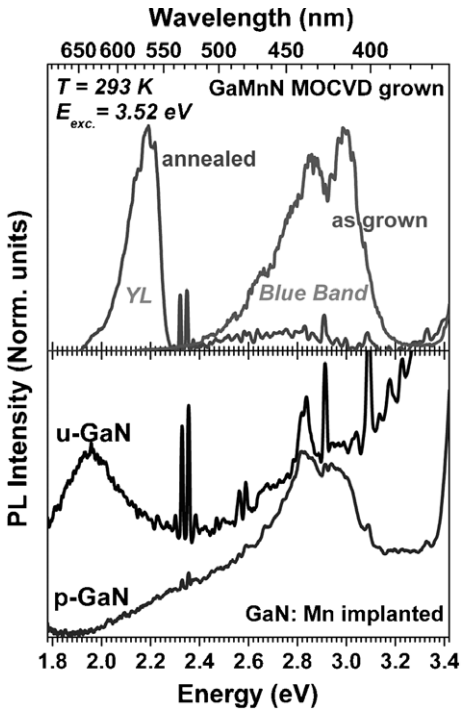

Figure 3. Photoluminescence spectra from MOCVD grown and implanted $Ga_{1-x}Mn_xN$ samples. A Mn-related transition occurs at ∼3.0 eV, while the other transitions such as the yellow luminescence (YL) and the low-energy tail of the blue luminescence band (BL) can also be found in the template layer. The latter emissions are assigned either to crystalline defects (e.g., Ga vacancies) in the case of the YL or donor-acceptor transitions (BL) typically seen in compensated p-doped GaN.

respective band observed for compensated GaN:Mg, where different defect bands involving spatially indirect transitions were resolved to contribute to the blue emission band [20]. Following the annealing process, the dominate feature (yellow band emission) in these spectra is commonly attributed to defect centres (e.g., Ga vacancies [21]) in the GaN buffer layer and the epilayer. The decrease in intensity of the yellow band in sample C prior to annealing is attributed to the enhanced Mn incorporation; this is in good agreement with previous reports [16, 17]. The transmission experiments (not shown here) revealed for the thick sample C an increase of detected light below 2.7 eV and a very weak absorption signal around 1.75 eV. The latter is tentatively assigned to the emission of holes from the neutral Mn^{3+} acceptor state [22]. The increase in the transmission signal below 2.7 eV is in good agreement with the observed PL band around 3.0 eV and suggests resonant absorption by Mn-related states [7]. For the implanted samples, the blue luminescence band is still visible in the implanted p-GaN sample, whereas the most prevalent feature in the implanted undoped sample is a broad emission band near the yellow, as seen in the annealed sample. As shown below, there is a correlation between the presence of these emission bands and the strength of the magnetic signal.

The macroscopic magnetization behaviour of the films was determined by temperature-dependent SQUID magnetometry on undoped and Mn-doped samples from 5 K to 300 K. A perspicuous magnetic hysteresis was obtained in samples C and E, providing a clear evidence for the

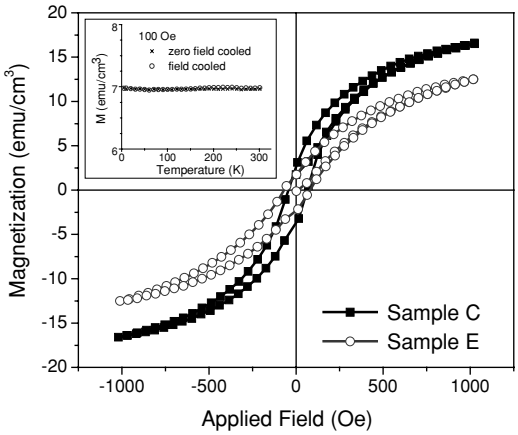

Figure 4. Room temperature hysteresis loop as measured in $Ga_{1-x}Mn_xN$ samples C ($x = 0.01$) and E ($x = 0.015$) grown by metalorganic chemical vapour deposition. The inset shows zero field cooled and field cooled magnetization curves for sample C taken at 100 Oe.

room temperature ferromagnetic properties shown in figure 4. A coercivity of 70 Oe and saturation magnetization of 11.6 emu cm^{-3} is observed in sample C at 300 K. This magnetization value results in a magnetic contribution per Mn atom of approximately 2.9 μ_B, which is similar to values observed in high-quality lightly doped $Ga_{1-x}Mn_xN$ produced by other methods [23, 24]. As doping increases, the magnetic signature per Mn atom decreases (to 1.3 μ_B/Mn in sample E) due to the formation of Mn-related compensating defects, as has been previously observed in $Ga_{1-x}Mn_xAs$ [25]. Note that ferromagnetism was achieved despite both the Mn and free hole concentration being far lower than that required by the mean-field theory [1]. The temperature dependence of the zero-field cooled and field cooled curves (shown in the inset of figure 4) indicates that the T_C of the magnetic phase is well above room temperature. A comparison of the zero field cooled and field cooled magnetization plots at 100 Oe showed no evidence for superparamagnetic clusters as the source of the observed hysteresis. Upon annealing, the magnetic signature decreases; similarly, a stark difference in magnetic signature is also seen between p-type and intrinsic GaN layers under the same implanting and annealing conditions as reported elsewhere [26]. It appears that the blue-band luminescence seen in these two samples is related to this state, which results in stronger ferromagnetic behaviour in the $Ga_{1-x}Mn_xN$ system.

Although no direct evidence of metallic GaMn- or MnN-clusters was observed in high-resolution XRD, the presence of small ferromagnetic clusters or additional phases could not be completely ruled out. Small size or small volume fraction or an orientation along non-*c*-axis directions would suppress the respective signals. Hence, the experimental findings do not fully preclude the existence of these second phases below the resolution limit of the XRD instrument. Based on the contribution per Mn atom, however, this is unlikely to be the sole source of ferromagnetism. In addition, the cluster model cannot explain differences in the strength of the magnetization with annealing or in the p-type and n-type implanted samples. Formation of manganese nitride compounds has also been seen in bulk crystals of $Ga_{1-x}Mn_xN$ [15] and annealed samples of Mn-implanted GaN [27].

Hall measurements indicated that the as-grown $Ga_{1-x}Mn_xN$ is semi-insulating. Co-doping with other shallow dopants or acceptors does not improve the conductivity significantly, which is consistent with the report of Mn as a deep trap [22]. A different origin of the ferromagnetism has to be considered since no p-type conductivity was observed, in contradiction to predictions of prevailing mean-field DMS theories. This lack of agreement with the DMS mean-field theories is often reported for ferromagnetism in the III nitrides. Alternately, the ferromagnetism may be related to a Mn-related impurity band within the bandgap resulting from double exchange as also be suggested via density functional theory calculations [28]. This model does not require additional carriers, and predicts elevated (above RT) Curie temperatures for even low (2%) Mn concentrations. Theoretical predictions also anticipate large T_C values for MnN clusters in the nitride-based materials [3], which could play at least a small role in these samples. The elevated growth temperatures in MOCVD promote enhanced surface and bulk diffusion and hence may lead to more Mn–Mn and Mn–N interactions than in samples produced by lower growth-temperature methods.

4. Conclusions

$Ga_{1-x}Mn_xN$ has been grown by metalorganic chemical vapour deposition with lattice-level incorporation of manganese. The system exhibits magnetic hysteresis in the as-grown material. Photoluminescence measurements indicate the presence of Mn-related defect states providing transitions near 3.0 eV. This Mn-related blue band luminescence correlates with samples exhibiting stronger ferromagnetic behaviour in both implanted and MOCVD-grown samples. Based on these preliminary results, MOCVD is likely to provide a method for future *in situ* integration of ferromagnetic semiconductor materials into devices.

Acknowledgments

This work was supported in part by grants from the Air Force Office of Scientific Research (T Steiner) and National Science Foundation (ECS 0224266). One author (MK) was supported by a National Defense Science and Engineering Graduate Fellowship sponsored by the Department of Defense. MS gratefully acknowledges the fellowship of the Alexander von Humboldt-foundation. The authors are grateful to A M Payne, D Nicol, D Mehta, and K Shalini for assistance with some of the measurements.

References

[1] Dietl T, Ohno H, Matsukura F, Cibert J and Ferrand D 2000 *Science* **287** 1019
[2] van Schilfgaarde M and Myrasov O N 2001 *Phys. Rev.* B **63** 233205
[3] Rao B K and Jena P 2002 *Phys. Rev. Lett.* **89** 185504
[4] Sato K and Katayama-Yoshida H 2002 *Semicond. Sci. Technol.* **17** 367
[5] Kronik L, Jain M and Chelikowsky J R 2002 *Phys. Rev.* B **66** 041203

[6] Reed M L, El-Masry N A, Stadelmaier H H, Ritums M K, Reed M J, Parker C A, Roberts J C and Bedair S M 2001 *Appl. Phys. Lett.* **79** 3473
[7] Polyakov A Y, Smirnov N B, Govorkov A V, Pashkova N Y, Kim J, Ren F, Overberg M E, Thaler G T, Abernathy C R, Pearton S J and Wilson R G 2002 *J. Appl. Phys.* **92** 3130
[8] Kuwabara S, Ishii K, Haneda S, Kondo T and Munekata H 2001 *Physica* E **10** 233
[9] Sonoda S, Hori H, Yamamoto Y, Sasaki T, Sato M, Shimizu S, Suga K-I and Kindo K 2002 *IEEE Trans. Magn.* **38** 2859
[10] Korotkov R Y, Gregie J M and Wessels B W 2001 *Mater. Res. Soc. Symp. Proc.* **639** G3.7.1
[11] Ando K 2003 *Appl. Phys. Lett.* **82** 100
[12] Dhar S, Brandt O, Trampert A, Daweritz L, Friedland K J, Ploog K H, Keller J, Beschoten B and Guntherodt G 2003 *Appl. Phys. Lett.* **82** 2077
[13] Thaler G T, Frazier R M, Stapleton J, Abernathy C R, Pearton S J, Kelly J, Rairigh R, Hebard A F and Zavada J M 2004 *Electrochem. Solid State Lett.* **7** G34
[14] Hashimoto M, Zhou Y K, Tampo H, Kanamura M and Asahi A 2003 *J. Cryst. Growth* **252** 499
[15] Zajac M, Doradzinski R, Gosk J, Szczytko J, Lefeld-Sosnowska M, Kaminska M, Twardowski A, Palczewska M, Grzanka E and Gebicki W 2001 *Appl. Phys. Lett.* **78** 1276
[16] Shon Y, Kwon Y H, Yuldashev S U, Leem J H, Park C S, Fu D J, Kim H J, Kang T W and Fan X J 2002 *Appl. Phys. Lett.* **81** 1845
[17] Xu J, Li J, Zhang R, Xiu X Q, Lu D Q, Gu S L, Shen B, Shi Y and Zheng Y D 2002 *Mater. Res. Soc. Symp. Proc.* **693** 207
[18] Baik J M, Lee J-L, Shon Y and Kang T W 2003 *J. Appl. Phys.* **93** 9024
[19] Yoon I T, Park C S, Kim H J, Kim Y G, Kang T W, Jeong M C, Ham M H and Myoung J M 2004 *J. Appl. Phys.* **92** 3130
[20] Han B, Gregie J M and Wessels B W 2003 *Phys. Rev.* B **68** 045205
[21] Monemar B 1998 *J. Cryst. Growth* **189** 1
[22] Graf T, Gjukic M, Brandt M S, Stutzmann M and Ambacher O 2002 *Appl. Phys. Lett.* **81** 5159
[23] Reed M L, Berkman E A, Reed M J, Arkun F E, Chikyow T, Bedair S M, Zavada J M and El-Masry N A 2004 *Mater. Res. Soc. Symp. Proc.* **798** Y8.6.1
[24] Kuroda S, Bellet-Amalric E, Biquard X, Cibert J, Giraud R, Marcet S and Mariette H 2003 *Phys. Status Solidi* b **240** 443
[25] Potashnik S J, Ku K C, Mahendiran R, Chun S H, Wang R F, Samarth N and Schiffer P 2002 *Phys. Rev.* B **66** 012408
[26] Kane M H, Asghar A, Payne A M, Vestal C R, Zhang Z J, Strassburg M, Senawirante J, Dietz N, Summers C J and Ferguson I T 2004 *Phys. Status Solidi* c at press
[27] Baik J M, Jang H W, Kim J K and Lee J-L 2003 *Appl. Phys. Lett.* **82** 583
[28] Sato K, Dederichs P H, Katayama-Yoshida H and Kudrnovsky J 2003 *Physica* B **340–342** 863